This is an open access article published under a Creative Commons Attribution (CC-BY) License, which permits unrestricted use, distribution and reproduction in any medium, provided the author and source are cited.

Inorganic Chemistry

Communication

pubs.acs.org/IC

Iridium Cyclooctene Complex That Forms a Hyperpolarization Transfer Catalyst before Converting to a Binuclear C−H Bond Activation Product Responsible for Hydrogen Isotope Exchange

Wissam Iali, Gary G. R. Green, Sam J. Hart, Adrian C. Whitwood, and Simon B. Duckett*

Centre for Hyperpolarization in Magnetic Resonance, University of York, York YO10 3NR, U.K.

Supporting Information

ABSTRACT: $[IrCl(COE)_2]_2$ (**1**) reacts with pyridine (py) and H_2 to form crystallographically characterized $IrCl(H)_2(COE)(py)_2$ (**2**). **2** undergoes py loss to form 16-electron $IrCl(H)_2(COE)(py)$ (**3**), with equivalent hydride ligands. When this reaction is studied with parahydrogen, **1** efficiently achieves hyperpolarization of free py (and nicotinamide, nicotine, 5-aminopyrimidine, and 3,5-lutudine) via signal amplification by reversible exchange (SABRE) and hence reflects a simple and readily available precatayst for this process. **2** reacts further over 48 h at 298 K to form crystallographically characterized $(Cl)(H)(py)$-$(\mu$-$Cl)(\mu$-$H)(\kappa$-μ-$NC_5H_4)Ir(H)(py)_2$ (**4**). This dimer is active in the hydrogen isotope exchange process that is used in radiopharmaceutical preparations. Furthermore, while $[Ir(H)_2(COE)(py)_3]PF_6$ (**6**) forms upon the addition of $AgPF_6$ to **2**, its stability precludes its efficient involvement in SABRE.

Nuclear Magnetic Resonance (NMR) spectroscopy is used widely in chemistry and biochemistry to characterize materials, while in medicine, magnetic resonance imaging is used to probe disease. Both methods suffer from low sensitivity, that can be overcome by employing hyperpolarization as exemplified by optical pumping,[1] dynamic nuclear polarization (DNP),[2] and parahydrogen (p-H_2).[3] The resulting molecules are starting to be featured as disease probes in clinical diagnosis.[4]

Parahydrogen-induced polarization (PHIP) involves the chemical transfer of two hydrogen atoms into a suitable acceptor.[5] This approach was pioneered by Bowers and Weitekamp,[3] Eisenberg et al.,[6] and Natterer and Bargon.[7] Examples of hydrogen acceptors include organic scaffolds leading to fumaric acid[8] and inorganic complexes such as the Vaska's complex.[9] One related PHIP approach, is known as signal amplification by reversible exchange (SABRE).[10] Like PHIP, it is able to hyperpolarize a target in seconds, but crucially it no longer involves the incorporation of p-H_2 into it. Instead, it utilizes a metal complex to simultaneously bind p-H_2, and the hyperpolarization target. When so assembled, polarization flows from the p-H_2-derived spins at low magnetic field to those of the target, which upon dissociation can be detected with high sensitivity.

Crabtree's catalyst, $[Ir(COD)(PCy_3)(py)][BF_4]$ (COD = cyclooctadiene, Cy = cyclohexyl, and py = pyridine), exhibits roles in hydrogenation[11] and hydrogen isotope exchange (HIE),[12] where it is used in the production of labeled compounds and radiopharmaceuticals.[13] When it reacts with p-H_2 and py though, it forms the active magnetization transfer catalyst $[Ir(H)_2(PCy_3)(py)_3][BF_4]$.[14] Interrogation of the free py's ^{1}H NMR signals after magnetization transfer revealed signal enhancements of >100-fold in the corresponding ^{1}H, ^{13}C, and ^{15}N NMR spectra. This process has now been refined to extend the level of signal gain,[15−18] the range of applications,[19,20] the nuclei that can be polarized,[21−25] and the classes of substrates that can be employed.[26−28] So far, IrCl(COD)(IMes)[29] [IMes = 1,3-bis(2,4,6-trimethylphenyl)imidazole-2-ylidene][4] reflects one of the better SABRE catalysts because its ligand exchange rates match those of the spin-spin couplings associated with polarization flow, but slow catalyst activation can be a problem.[30,31] We set out here to develop a rapidly activating and readily available air-stable precursor for SABRE and now describe the ensuing observations.

Initially, the COD ligand of IrCl(COD)(IMes) was replaced with cyclooctene (COE), in the form of $IrCl(COE)_2(IMes)$,[32] by adding IMes to $[IrCl(COE)_2]_2$ (**1**). $IrCl(COE)_2(IMes)$ proved unstable, although $[Ir(H)_2(IMes)(py)_3][Cl]$ forms upon reaction with py and H_2. As a consequence, we treated a tetrahydrofuran (THF-d_8) solution of **1** with py and H_2 alone. **1** rapidly formed $IrCl(H)_2(\eta^2$-COE$)(py)_2$ (**2**), as detailed in Figure 1.

The COE ligand of **2** binds in an η^2 fashion, trans to one of two inequivalent py ligands, while its hydride ligands lie trans to chloride and py. The py-N1−iridium alkene centroid bond angle in **2** is 101.6(6)°, while the py−iridium chlorine bond angles are 91.1(3)° and 92.4(3)°. Its structure is therefore close to octahedral, although the py ligand cis to the alkene is slightly

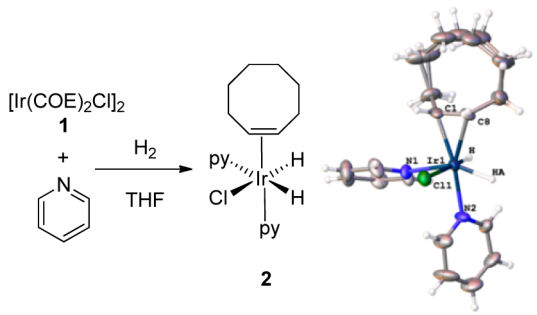

Figure 1. Reaction scheme for the formation of **2** from **1** and the associated ORTEP for **2**.

Received: October 24, 2016
Published: November 9, 2016

 © 2016 American Chemical Society

DOI: 10.1021/acs.inorgchem.6b02560
Inorg. Chem. 2016, 55, 11639−11643

displaced away from the equatorial plane. The corresponding alkene C1−Ir and C8−Ir bonds lengths are 2.152(11) and 2.187(10) Å, respectively, and compare with those of 2.1664(13) and 2.1494(14) Å in (η^2-COE)(Me)Ir(PMe_3)$_3$[33] and 2.2865(7) and 2.307(7) Å [(^{i}PrN-PCP)IrHCl(COE)].[34] The Ir−N1 and Ir−N2 bond lengths of **2** are 2.216(9) and 2.106(8) Å, respectively, in accordance with the trans-labilizing influence of hydride and compare with those of 2.192(3) and 2.129(3) Å in [Ir(H)$_2$IMes(py)$_3$]Cl for sites trans to hydride and carbene, respectively.[35]

The ^{1}H NMR spectrum of **2** contains hydride ligand signals at δ −19.34 and −26.47 for sites trans to py and chloride, respectively, and two inequivalent CH proton signals for the COE ligand at δ 3.12 and 4.12. The ^{15}N chemical shifts of its py ligands appear at $\delta_{py\text{-}eq}$ 254.7 and $\delta_{py\text{-}ax}$ 224.7, with the former exhibiting a large J_{H15N} splitting of 20 Hz due to a trans hydride ligand coupling. Diagnostic α-proton signals for these ligands appear at δ 9.37 and 9.25, respectively, with the low-field ^{15}N axial py chemical shift reflecting its shorter iridium bond length.[36]

The ligands of **2** proved to exhibit dynamic effects that were quantified by exchange spectroscopy (EXSY) methods (Supporting Information). The rate of py loss for the equatorial site was determined to be 7.8 ± 0.1 s^{-1} at 298 K, and hydride site exchange into free H$_2$ proved to be limited at this temperature. In contrast, the two distinct hydride sites of **2** proved to interchange positions at a rate of 3.6 ± 0.1 s^{-1}, while the CH proton sites of COE interconvert at a rate of 3.8 ± 0.1 s^{-1}. When the concentrations of py and H$_2$ were varied (see sTable 1). None of the associated ligand exchange rates changed. Further samples were then examined that contained excesses of COE and Cl$^-$ (in the form of [^{t}Bu$_4$C]Cl) in addition to py and H$_2$, and no change in the rate was observed. Hence py dissociation from the site trans to hydride forms intermediate IrCl(H)$_2$(COE)(py) (**3**) of Scheme 1 with equivalent hydrides. For symmetry reasons,

Scheme 1. Ligand-Exchange Pathways Observed by NMR for 2 in a THF-d_8 Solution

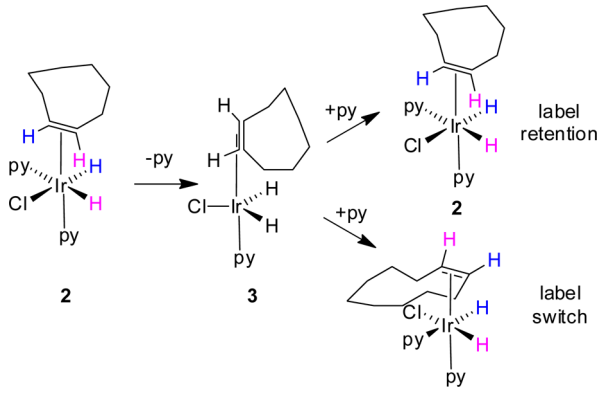

reformation of **2** proceeds with interchange of the original hydride and alkene CH proton sites at approximately 50% of the py loss rate. In agreement with this conclusion, Eyring analysis of this behavior as a function of the temperature produces three slopes with identical gradients. The corresponding activation parameters for py loss are $\Delta H^{\ddagger}$ = 90.6 ± 1 kJ mol^{-1} and $\Delta S^{\ddagger}$ = 79 ± 4 J K^{-1} mol^{-1} and reflect the dissociative nature of this change.

When the H$_2$ gas used in these control experiments was replaced by D$_2$, a loss of the hydride ligand signals of **2** was observed over a few seconds, with slow ^{2}H incorporation into the bound cyclooctene CH═ groups being evident at a rate of 1.3 (±0.5) × 10^{-5} s^{-1}. Furthermore, when p-H$_2$ is used, the corresponding hydride ligand signals exhibit the PHIP effect, as detailed in Figure 2. These observations confirm that **2**

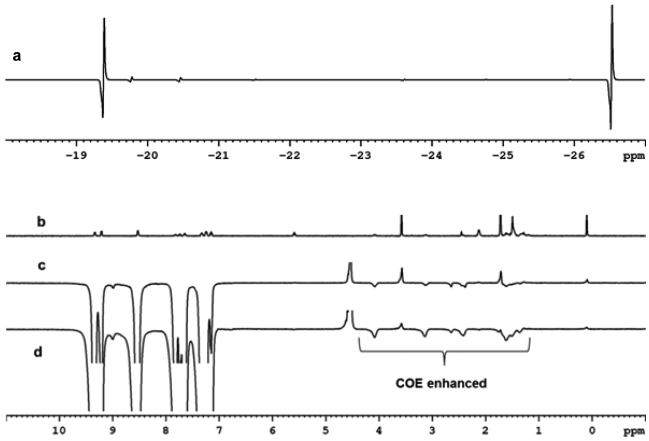

Figure 2. Hyperpolarized ^{1}H NMR spectra of **2**. (a) Hydride region showing PHIP-enhanced signals for cis−cis **2** and its minor cis−trans isomer (298 K). Organic region showing (b) the normal spectrum, (c) SABRE-enhanced free and bound py signals (298 K), and (d) SABRE-enhanced signals for the COE ligand of **2** (313 K).

undergoes reversible H$_2$ loss, and when the same sample was exposed to p-H$_2$ in a low magnetic field for 10 s prior to making the high-field NMR measurement, the SABRE effect was observed. Figure 2b shows this as viewed through the +11 to −1 ppm region of the NMR spectrum for a sample containing 1 equiv of free py relative to **2**. The bound py and COE proton signals referred to earlier are now hyperpolarized, and consequently **2** represents a catalyst for SABRE.

The degree of SABRE shown in these resonances depends on the excess of py. When the initial ratio of **1** to py was 1:8, a >210-fold intensity gain in the ortho proton resonance of the free py signal is observed. This enhancement increases to >500-fold when the ligand ratio is 1:5.6 and can be increased further by warming to 313 K; sTable 4 contains data for nicotinamide, nicotine, 5-aminopyrimidine, and 3,5-lutudine to demonstrate scope. However, after the sample is left at 298 K for 24 h, three new hydride signals appear in the corresponding ^{1}H NMR spectra at δ −24.72, −25.9, and −28.95 for (Cl)(H)(py)(μ-Cl)(μ-H)(κ-μ-NC$_5$H$_4$)Ir(H)(py)$_2$ (**4**). Their intensity growth parallels a series of changes in the aromatic region of these NMR spectra, which suggests that **4** contains four distinct py-based ligands. Integration and COSY measurements show that one of these has just four protons and hence **4** is the C−H bond activation product (Cl)(H)(py)(μ-Cl)(μ-H)(κ-μ-NC$_5$H$_4$)Ir(H)(py)$_2$ of Figure 3.

The distance between the two iridium centers of **4** is 2.73319(18) Å, while the corresponding Ir−C and Ir−N bond lengths of the bridging pyridyl moiety are 1.998(3) Å and 2.013(3) Å, respectively. A related iridium dimer studied by Cotton and Poli[37] had analogous Ir−C and Ir−N bond lengths of 1.983(13) and 2.024(12) Å, respectively, with an Ir−Ir distance of 2.518(1) Å. The Ir1−N2, Ir1−Cl2, and Ir1−Cl1 bond lengths are 2.068(3), 2.3897(8), and 2.5732(8) Å, respectively, in accordance with the asymmetry in the bridging chloride. The corresponding Ir2−N4, Ir2−N3, and terminal Ir2−Cl2 bond lengths are 2.152(3), 2.072(3), and 2.5579(8) Å, respectively, with the hydride ligands again clearly exhibiting a trans-labializing influence, although the Ir−N bond lengths are all

DOI: 10.1021/acs.inorgchem.6b02560
Inorg. Chem. 2016, 55, 11639−11643

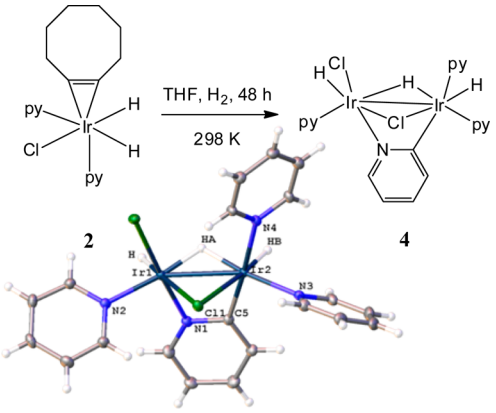

Figure 3. Reaction scheme for the formation of **4** alongside an ORTEP of **4**.

shorter than those of the labile site in **2**. The key bond angles for Ir1, N2−Ir1−Cl2, Cl2−Ir1−Cl1, and N1−Ir1−Cl1, are 86.92(8)°, 93.72(3)°, and 84.45(8)°, respectively, while those for Ir2, N3−Ir2−Cl1, C5−Ir2−Cl1, and N4−Ir2−Cl1, are 98.53(8)°, 85.38(10)°, and 92.89(8)°, respectively. The ligand arrangement around both iridium centers is therefore close to octahedral.

Complex **4** is SABRE inactive and its hydride ligand signals fail to exhibit PHIP. However, when **4** is shaken with **2** under *p*-H_2, the ^{1}H NMR signals of free py are enhanced alongside those for the bound py ligands of **4**, which provide ortho proton signals at δ 9.48 and 9.40, which suggests that ligand exchange is possible. The addition of pyridine-d_5 to the ^{1}H-labeled **4** under H_2 at 273 K confirms this effect, with the order of ligand exchange based on the fall in the ortho proton site resonance intensities being δ 9.40 > δ 9.48 ≫ δ 9.33, as detailed in Figure 4. We note that the

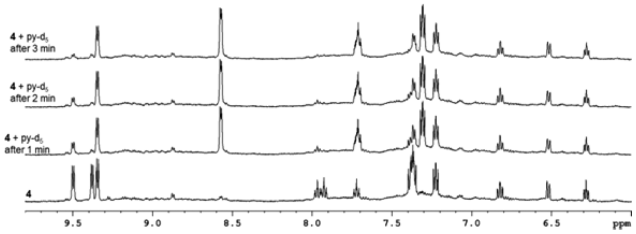

Figure 4. Intensity fall of appropriate ^{1}H NMR resonances in ^{1}H-containing **4** at 273 K upon exposure to pyridine-d_5 revealing the slow and selective exchange of its py-based ligands.

corresponding Ir−N bond lengths for these groups are 2.068(3), 2.072(3), and 2.152(3) Å, respectively, and fit with these observations. Exchange of the pyridyl ligand with pyridine-d_5 proved to be slower still.

In addition to these changes, the slow replacement of the ^{2}H labels of pyridine-d_5 with ^{1}H nuclei is observed. After 48 h at 313 K, 33% of its ortho py ^{2}H sites became ^{1}H containing, with 5.4% incorporation into the para site and 3.1% into the meta site. **4** therefore facilitates py CH/CD exchange through transfer from D_2/H_2.[12] When 3 bar of D_2 was employed with a pyridine-h_5 to **4** ratio of 25:1, the rate of ^{2}H label incorporation proved to be 4.3×10^{-5} s^{-1} (ortho), 3.85×10^{-5} s^{-1} (meta), and 3.05×10^{-5} s^{-1} (para) at 313 K.

Given the SABRE activity of $[Ir(H)_2(PCy_3)(py)_3][BF_4]$ referred to earlier, we added $AgPF_6$ to **2** to form $[Ir(H)_2(COE)(py)_3]PF_6$ (**6**) of Scheme 2. **6** was also prepared independently

Scheme 2. Routes to 6

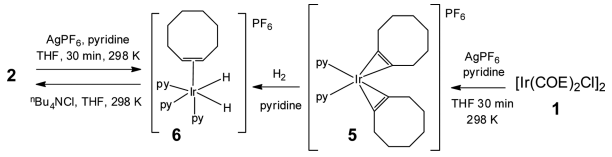

from $[Ir(COE)_2(py)_2]PF_6$ (**5**; Supporting Information). It proved to be SABRE-inactive at 298 K, in agreement with the py loss rate of 0.007 s^{-1}; warming to 313 K produces limited SABRE, but the bound py signals are stronger than those of free py. **6** is therefore unsuited to SABRE, with the small ligand loss rate being consistent with the reduced steric effect of this ligand relative to PCy_3.

In summary we have established that readily available air-stable **1** reacts with py and H_2 to form **2**. **2** is highly effective for hyperpolarization of py via the SABRE effect in nonprotoic solvents and with its simple alkene coligand far easier to employ than the carbene complexes more usually used. When this process is undertaken with nicotinamide, nicotine, 5-amino-pyrimidine, and 3,5-lutudine, good levels of SABRE are seen. Hence, **1** reflects a simple and readily available precatayst for this process.

Over 48 h, **2** reacts to form the novel C−H bond activation product **4** in a reaction inhibited by added py. This novel complex exhibits catalytic activity in the HIE reaction, which is used for the site-specific labeling of drugs. The presented results offer insight into the HIE process and suggest how ligand design might be used to improve its efficiency in the future. In addition, the high-field one-proton PHIP effect of Permin and Eisenberg[38] uses the chemical transfer of a single proton previously located in a molecule of *p*-H_2 to enable its detection as a hyperpolarized signal in an organic species.[38,39] While slow-reacting **4** does not behave in this way, its detection suggests that faster-reacting systems will show PHIP at high field.[40]

■ ASSOCIATED CONTENT

Supporting Information

The Supporting Information is available free of charge on the ACS Publications website at DOI: 10.1021/acs.inorgchem.6b02560.

Complex synthesis and NMR spectra (PDF)

X-ray crystallographic data in CIF format for **2** (CIF)

X-ray crystallographic data in CIF format for **4** (CIF)

X-ray crystallographic data in CIF format for **5** (CIF)

■ AUTHOR INFORMATION

Corresponding Author

*E-mail: simon.duckett@york.ac.uk.

Notes

The authors declare no competing financial interest.

Raw NMR data can be found at DOI: 10.15124/b79561d6-be21-4ca9-8975-4be9eb0c43b6.

■ ACKNOWLEDGMENTS

We thank the Wellcome Trust for funding (Grants 092506 and 098335).

DOI: 10.1021/acs.inorgchem.6b02560
Inorg. Chem. 2016, 55, 11639−11643

REFERENCES

(1) Albert, M. S.; Cates, G. D.; Driehuys, B.; Happer, W.; Saam, B.; Springer, C. S.; Wishnia, A. Biological Magnetic-Resonance-Imaging Using Laser Polarized Xe-129. *Nature* **1994**, *370* (6486), 199−201.

(2) Ardenkjaer-Larsen, J. H.; Fridlund, B.; Gram, A.; Hansson, G.; Hansson, L.; Lerche, M. H.; Servin, R.; Thaning, M.; Golman, K. Increase in signal-to-noise ratio of > 10,000 times in liquid-state NMR. *Proc. Natl. Acad. Sci. U. S. A.* **2003**, *100* (18), 10158−10163.

(3) Bowers, C. R.; Weitekamp, D. P. Para-Hydrogen and Synthesis Allow Dramatically Enhanced Nuclear Alignment. *J. Am. Chem. Soc.* **1987**, *109* (18), 5541−5542.

(4) Kurhanewicz, J.; Vigneron, D. B.; Brindle, K.; Chekmenev, E. Y.; Comment, A.; Cunningham, C. H.; DeBerardinis, R. J.; Green, G. G.; Leach, M. O.; Rajan, S. S.; Rizi, R. R.; Ross, B. D.; Warren, W. S.; Malloy, C. R. Analysis of Cancer Metabolism by Imaging Hyperpolarized Nuclei: Prospects for Translation to Clinical Research. *Neoplasia* **2011**, *13* (2), 81−97.

(5) Green, R. A.; Adams, R. W.; Duckett, S. B.; Mewis, R. E.; Williamson, D. C.; Green, G. G. R. The theory and practice of hyperpolarization in magnetic resonance using parahydrogen. *Prog. Nucl. Magn. Reson. Spectrosc.* **2012**, *67*, 1−48.

(6) Eisenschmid, T. C.; Kirss, R. U.; Deutsch, P. P.; Hommeltoft, S. I.; Eisenberg, R.; Bargon, J.; Lawler, R. G.; Balch, A. L. Para Hydrogen Induced Polarization in Hydrogenation Reactions. *J. Am. Chem. Soc.* **1987**, *109* (26), 8089−8091.

(7) Natterer, J.; Bargon, J. Parahydrogen induced polarization. *Prog. Nucl. Magn. Reson. Spectrosc.* **1997**, *31*, 293−315.

(8) Chekmenev, E. Y.; Hovener, J.; Norton, V. A.; Harris, K.; Batchelder, L. S.; Bhattacharya, P.; Ross, B. D.; Weitekamp, D. P. PASADENA hyperpolarization of succinic acid for MRI and NMR spectroscopy. *J. Am. Chem. Soc.* **2008**, *130* (13), 4212−4213.

(9) Hasnip, S. K.; Duckett, S. B.; Sleigh, C. J.; Taylor, D. R.; Barlow, G. K.; Taylor, M. J. New products in an old reaction: isomeric products from H-2 addition to Vaska's complex and its analogues. *Chem. Commun. (Cambridge, U. K.)* **1999**, No. 17, 1717−1718.

(10) Adams, R. W.; Aguilar, J. A.; Atkinson, K. D.; Cowley, M. J.; Elliott, P. I. P.; Duckett, S. B.; Green, G. G. R.; Khazal, I. G.; Lopez-Serrano, J.; Williamson, D. C. Reversible Interactions with para-Hydrogen Enhance NMR Sensitivity by Polarization Transfer. *Science* **2009**, *323* (5922), 1708−1711.

(11) Crabtree, R. IRIDIUM COMPOUNDS IN CATALYSIS. *Acc. Chem. Res.* **1979**, *12* (9), 331−338.

(12) Ellames, G. J.; Gibson, J. S.; Herbert, J. M.; McNeill, A. H. The scope and limitations of deuteration mediated by Crabtree's catalyst. *Tetrahedron* **2001**, *57* (46), 9487−9497.

(13) Nilsson, G. N.; Kerr, W. J. The development and use of novel iridium complexes as catalysts for ortho-directed hydrogen isotope exchange reactions. *J. Labelled Compd. Radiopharm.* **2010**, *53* (11−12), 662−667.

(14) Atkinson, K. D.; Cowley, M. J.; Elliott, P. I. P.; Duckett, S. B.; Green, G. G. R.; Lopez-Serrano, J.; Whitwood, A. C. Spontaneous Transfer of Parahydrogen Derived Spin Order to Pyridine at Low Magnetic Field. *J. Am. Chem. Soc.* **2009**, *131* (37), 13362−13368.

(15) Lloyd, L. S.; Asghar, A.; Burns, M. J.; Charlton, A.; Coombes, S.; Cowley, M. J.; Dear, G. J.; Duckett, S. B.; Genov, G. R.; Green, G. G. R.; Highton, L. A. R.; Hooper, A. J. J.; Khan, M.; Khazal, I. G.; Lewis, R. J.; Mewis, R. E.; Roberts, A. D.; Ruddlesden, A. J. Hyperpolarisation through reversible interactions with parahydrogen. *Catal. Sci. Technol.* **2014**, *4* (10), 3544−3554.

(16) Eshuis, N.; Hermkens, N.; van Weerdenburg, B. J. A.; Feiters, M. C.; Rutjes, F.; Wijmenga, S. S.; Tessari, M. Toward Nanomolar Detection by NMR Through SABRE Hyperpolarization. *J. Am. Chem. Soc.* **2014**, *136* (7), 2695−2698.

(17) Theis, T.; Truong, M. L.; Coffey, A. M.; Shchepin, R. V.; Waddell, K. W.; Shi, F.; Goodson, B. M.; Warren, W. S.; Chekmenev, E. Y. Microtesla SABRE Enables 10% Nitrogen-15 Nuclear Spin Polarization. *J. Am. Chem. Soc.* **2015**, *137* (4), 1404−1407.

(18) Truong, M. L.; Theis, T.; Coffey, A. M.; Shchepin, R. V.; Waddell, K. W.; Shi, F.; Goodson, B. M.; Warren, W. S.; Chekmenev, E. Y. N-15 Hyperpolarization by Reversible Exchange Using SABRE-SHEATH. *J. Phys. Chem. C* **2015**, *119* (16), 8786−8797.

(19) Lloyd, L. S.; Adams, R. W.; Bernstein, M.; Coombes, S.; Duckett, S. B.; Green, G. G. R.; Lewis, R. J.; Mewis, R. E.; Sleigh, C. J. Utilization of SABRE-Derived Hyperpolarization To Detect Low-Concentration Analytes via 1D and 2D NMR Methods. *J. Am. Chem. Soc.* **2012**, *134* (31), 12904−12907.

(20) Eshuis, N.; van Weerdenburg, B. J. A.; Feiters, M. C.; Rutjes, F.; Wijmenga, S. S.; Tessari, M. Quantitative Trace Analysis of Complex Mixtures Using SABRE Hyperpolarization. *Angew. Chem., Int. Ed.* **2015**, *54* (5), 1481−1484.

(21) Mewis, R. E.; Atkinson, K. D.; Cowley, M. J.; Duckett, S. B.; Green, G. G. R.; Green, R. A.; Highton, L. A. R.; Kilgour, D.; Lloyd, L. S.; Lohman, J. A. B.; Williamson, D. C. Probing signal amplification by reversible exchange using an NMR flow system. *Magn. Reson. Chem.* **2014**, *52* (7), 358−369.

(22) Zhivonitko, V. V.; Skovpin, I. V.; Koptyug, I. V. Strong P-31 nuclear spin hyperpolarization produced via reversible chemical interaction with parahydrogen. *Chem. Commun. (Cambridge, U. K.)* **2015**, *51* (13), 2506−2509.

(23) van Weerdenburg, B. J. A.; Gloggler, S.; Eshuis, N.; Engwerda, A. H. J.; Smits, J. M. M.; de Gelder, R.; Appelt, S.; Wymenga, S. S.; Tessari, M.; Feiters, M. C.; Blumich, B.; Rutjes, F. Ligand effects of NHC-iridium catalysts for signal amplification by reversible exchange (SABRE). *Chem. Commun. (Cambridge, U. K.)* **2013**, *49* (67), 7388−7390.

(24) Barskiy, D. A.; Shchepin, R. V.; Coffey, A. M.; Theis, T.; Warren, W. S.; Goodson, B. M.; Chekmenev, E. Y. Over 20% N-15 Hyperpolarization in Under One Minute for Metronidazole, an Antibiotic and Hypoxia Probe. *J. Am. Chem. Soc.* **2016**, *138* (26), 8080−8083.

(25) Logan, A. W. J.; Theis, T.; Colell, J. F. P.; Warren, W. S.; Malcolmson, S. J. Hyperpolarization of Nitrogen-15 Schiff Bases by Reversible Exchange Catalysis with para-Hydrogen. *Chem. - Eur. J.* **2016**, *22* (31), 10777−10781.

(26) Zeng, H. F.; Xu, J. D.; Gillen, J.; McMahon, M. T.; Artemov, D.; Tyburn, J. M.; Lohman, J. A. B.; Mewis, R. E.; Atkinson, K. D.; Green, G. G. R.; Duckett, S. B.; van Zijl, P. C. M. Optimization of SABRE for polarization of the tuberculosis drugs pyrazinamide and isoniazid. *J. Magn. Reson.* **2013**, *237*, 73−78.

(27) Mewis, R. E.; Green, R. A.; Cockett, M. C. R.; Cowley, M. J.; Duckett, S. B.; Green, G. G. R.; John, R. O.; Rayner, P. J.; Williamson, D. C. Strategies for the Hyperpolarization of Acetonitrile and Related Ligands by SABRE. *J. Phys. Chem. B* **2015**, *119* (4), 1416−1424.

(28) Ducker, E. B.; Kuhn, L. T.; Munnemann, K.; Griesinger, C. Similarity of SABRE field dependence in chemically different substrates. *J. Magn. Reson.* **2012**, *214*, 159−165.

(29) Vazquez-Serrano, L. D.; Owens, B. T.; Buriak, J. M. Catalytic olefin hydrogenation using N-heterocyclic carbene-phosphine complexes of iridium. *Chem. Commun. (Cambridge, U. K.)* **2002**, No. 21, 2518−2519.

(30) Adams, R. W.; Duckett, S. B.; Green, R. A.; Williamson, D. C.; Green, G. G. R. A theoretical basis for spontaneous polarization transfer in non-hydrogenative parahydrogen-induced polarization. *J. Chem. Phys.* **2009**, *131* (19), 194505.

(31) Eshuis, N.; Aspers, R.; van Weerdenburg, B. J. A.; Feiters, M. C.; Rutjes, F.; Wijmenga, S. S.; Tessari, M. Determination of long-range scalar H-1-H-1 coupling constants responsible for polarization transfer in SABRE. *J. Magn. Reson.* **2016**, *265*, 59−66.

(32) Nelson, D. J.; Truscott, B. J.; Slawin, A. M. Z.; Nolan, S. P. Synthesis and Reactivity of New Bis(N-heterocyclic carbene) Iridium(I) Complexes. *Inorg. Chem.* **2013**, *52* (21), 12674−12681.

(33) Bleeke, J. R.; Thananatthanachon, T.; Rath, N. P. Silapentadienyl−Iridium−Phosphine Chemistry. *Organometallics* **2008**, *27* (11), 2436−2446.

(34) Brück, A.; Gallego, D.; Wang, W.; Irran, E.; Driess, M.; Hartwig, J. F. Pushing the σ-Donor Strength in Iridium Pincer Complexes: Bis(silylene) and Bis(germylene) Ligands Are Stronger Donors than Bis(phosphorus(III)) Ligands. *Angew. Chem., Int. Ed.* **2012**, *51* (46), 11478−11482.

DOI: 10.1021/acs.inorgchem.6b02560
Inorg. Chem. 2016, 55, 11639−11643

(35) Cowley, M. J.; Adams, R. W.; Atkinson, K. D.; Cockett, M. C. R.; Duckett, S. B.; Green, G. G. R.; Lohman, J. A. B.; Kerssebaum, R.; Kilgour, D.; Mewis, R. E. Iridium N-Heterocyclic Carbene Complexes as Efficient Catalysts for Magnetization Transfer from para-Hydrogen. *J. Am. Chem. Soc.* **2011**, *133* (16), 6134−6137.
(36) Pazderski, L. Application of N-15 NMR Spectroscopy to Determine Coordination Sphere Geometry in Pd(II), Pt(II), Pt(IV), CO(III) and Rh(III) Complexes with Azines. *Polym. J. Chem.* **2009**, *83* (7), 1241−1253.
(37) Cotton, F. A.; Poli, R. Synthesis and Molecular-Structure of a Dinuclear Quadruply Bridged Cobalt(Ii) Compound with a Short Metal Metal Bond, Co2[(P-Ch3c6h4)Nnnp-C6h4ch3)]4. *Inorg. Chem.* **1987**, *26* (22), 3652−3653.
(38) Permin, A. B.; Eisenberg, R. One-hydrogen polarization in hydroformylation promoted by platinum-tin and iridium carbonyl complexes: A new type of parahydrogen-induced effect. *J. Am. Chem. Soc.* **2002**, *124* (42), 12406−12407.
(39) Lopez-Serrano, J.; Duckett, S. B.; Aiken, S.; Almeida Lenero, K. Q.; Drent, E.; Dunne, J. P.; Konya, D.; Whitwood, A. C. A para-hydrogen investigation of palladium-catalyzed alkyne hydrogenation. *J. Am. Chem. Soc.* **2007**, *129* (20), 6513−6527.
(40) Barskiy, D. A.; Kovtunov, K. V.; Koptyug, I. V.; He, P.; Groome, K. A.; Best, Q. A.; Shi, F.; Goodson, B. M.; Shchepin, R. V.; Coffey, A. M.; Waddell, K. W.; Chekmenev, E. Y. The Feasibility of Formation and Kinetics of NMR Signal Amplification by Reversible Exchange (SABRE) at High Magnetic Field (9.4 T). *J. Am. Chem. Soc.* **2014**, *136* (9), 3322−3325.

DOI: 10.1021/acs.inorgchem.6b02560
Inorg. Chem. 2016, 55, 11639−11643